CRIS JUNCTIONS AND DEAD LAYERS

ACE Memo ID: 1997.02.08.BLD.a (JPL/CRIS/junction, dead layer)

From: Brian L. Dougherty (bld@heag1.jpl.nasa.gov)

To: CRIS Data Analysis Team

Date: 8 Feb. 1997

inre: We compare measurements of dead layers on CRIS detectors. Beams of fast argon nuclei and low-energy alphas were used. Discrepancies suggest a dependency on stopping power. The method that has produced all of our dead layer maps is found to be very sensitive to parameter errors. Alpha measurements indicate that charge-collection efficiencies vary with depth in the junctions. Arguments and calculations are offered (based on known fabrication procedures and charge transport physics) that help justify this last feature.

INTRODUCTION

Suppose a nucleus of charge Z and mass M enters a CRIS array, depositing energy in the planar silicon detectors which each have a thickness of $L \approx 3$ mm. If we approximate the stopping power as $dE/dx \propto Z^2(M/E)^{3/4}$, then the incident-particle mass resolution is related to uncertainties on detector thickness as $\partial M/M \approx 4\partial L/3L$. To achieve a 3-sigma (i.e. 99 %) separation of iron isotopes, L must be known to within about 7 µm. Such accuracy is needed for the depth of the active region as well as for the dead layers at each detector surface.

The aluminum and gold deposited on the junction and ohmic faces of our detectors are only a few hundred angstroms thick and therefore represent thin-window contacts. In contrast, dead layers are directly associated with diffused junctions on lithium-drifted silicon [Si(Li)] devices. This follows since the electric field strength within such a detector is not high everywhere, but abruptly drops to zero a short distance below one surface, at the "junction edge". Charge-carrier losses are greatest where field strengths are low, due to recombination, trapping, or absorption in the nearby metallic contact. Finally, charge-collection signals are strictly proportional to the relative field-induced separation of electrons and holes generated in an ionizing event.

The "junction depth" (at $x = w$) is that distance below the silicon surface (at $x = 0$) where the charge collection efficiency $\varepsilon(x)$ first reaches unity. This depth should correspond closely, but not necessarily exactly, to that distance where the electric field strength first becomes non-zero, which in turn is close to where the field reaches its maximum strength. As a corollary, $x = w$

should nearly match that depth at which the inversion of crystal "type" occurs; i.e. where the activated lithium density just drops below that of the acceptors present before compenation.

The naive dead-layer model of a junction posits that $\varepsilon = 0$ for any energy deposited at depths shallower than $x = w$, and $\varepsilon = 1$ for $x > w$. Since it is physically necessary for there to be a connected transition from $\varepsilon = 0$ to $\varepsilon = 1$, even if this transition region is very narrow compared with w, then dead-layers would be nearly identical with junctions. As will be described below, however, our alpha-particle data directly refutes this model.

With ε found to be non-zero in our junctions, dead-layer depths will equal $\delta L = fw$, where the weighting factor $f = 1 - \int_0^w \varepsilon(x)dx/w$. But f is not necessarily a unique value, as w is, since $\varepsilon(x)$ may depend on the density of energy deposited, which itself varies with the energy and species of penetrating particle. We will therefore compare dead layers derived from alpha-particle data with those due to beams of fast ^{36}Ar nuclei.

We will also breifly describe how diffused junctions are fabricated. Our model of varying ε with depth is then justified by known semiconductor physics arguments. Since that model is not unique, we will look at how our interpretations may be affected by the remaining ambiguities.

We note that Si(Li) detectors can be made using Schottky barriers; i.e. without diffused junctions, thus avoiding the dead layer issue. (The evaporated aluminum and gold contacts on each surface would be easily taken into account, and very thin.) But diffused junctions are easier to fabricate, and are much more stable (to temperature cycling) and robust (to changes occuring with surface damage).

MEASUREMENTS AT MICHIGAN STATE UNIVERSITY

We measured all CRIS detector thicknesses using an ^{36}Ar beam at MSU. Nuclei passed through one Si(Li) and stopped in another (see Figure 1), yielding ΔE and E' records of deposited energy respectively. Detectors were separated by 1 cm of air. The common normal to their surfaces was oriented 5° off the beam axis. By slowly rastering the beam, we mapped ΔE and E' at every location. Only three well-calibrated Si(Li) were used (repeatedly) for E' measurements. Nuclei entered the thin-window faces on both detectors, and stopped well before reaching the junction side of the E' detector. Thus there were no dead-layer losses in the E' data, but ΔE measurements did not include some energy deposited in the junctions of the penetrated detectors. Since this missing charge was generated at a known rate, corresponding to ^{36}Ar nuclei of energy E' passing through silicon, we could then calculate the total thicknesses of ΔE detectors using E' data, and find dead-layer thicknesses by analyzing E' and ΔE measurements together.

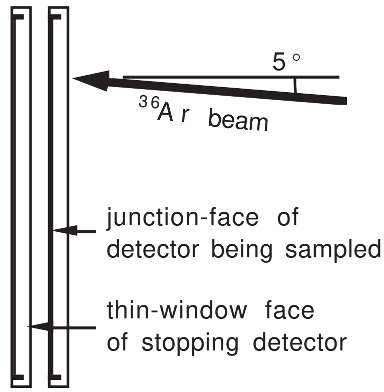

Figure1. Typical setup for measurements of detector thickness and dead layers at MSU.

The total beam energy did not need to be determined, but could be derived a-posteriori from the data if the gain was correctly calibrated. However, charge collection efficiency was not guarranteed to be unity everywhere within the detector bulk. Moreover, channelling was a minor but non-vanishing problem. If we ignore such ambiguities, though, the analysis can proceed straightforwardly. Absolute determinations of thickness (L) had already been made at several locations around each ΔE detector by using a capacitance meter that was reported to be accurate to within ± 1 μm. (The manufacturer, LBL, provided this data.) We then plot E' versus L measured at the same locations, and fit a line $L = L_o + mE'$, where L_o is a common offset and m is a proportionality: see Figure 2. From this fit we can find the total thickness at any other point. (We note that a "global" fit using L and E' measurements for all the detectors returns L_o and m values that differ very little from those shown.) Dead layers are then found through the following set of calculations:

$$\delta L = mE_{missing} - L_{air} \qquad E_{missing} = E_{tot} - (E' + \Delta E)$$

$$E_{tot} = (R_{tot}/k)^{1/a} \qquad R_{tot} = (L + L_{air})\sec\theta + R'$$

$$R' = k'E'^{a'} \qquad L = L_o + mE'$$

$$k = 3.23418\text{x}10^{-3} \qquad a = 1.7329$$

$$k' = 6.43773\text{x}10^{-3} \qquad a' = 1.6393$$

The angle θ nominally equals 5°. An airgap of 1 cm is equivalent to $L_{air} \approx 5$ μm of silicon. We employe power-law relationships to calculate residual range (R') in the E' detector, and the total energy (E_{tot}) deposited in both detectors and the intervening air. Parameters k and a are tuned for ranges calculable from E_{tot}. Likewise for k', a', and the residual energy E'. For the center of detector #8128 (which was used to make Figure 2) we have E' = 1170.6 MeV and ΔE = 1885.3 MeV, giving $\delta L \approx 42.3$ μm.

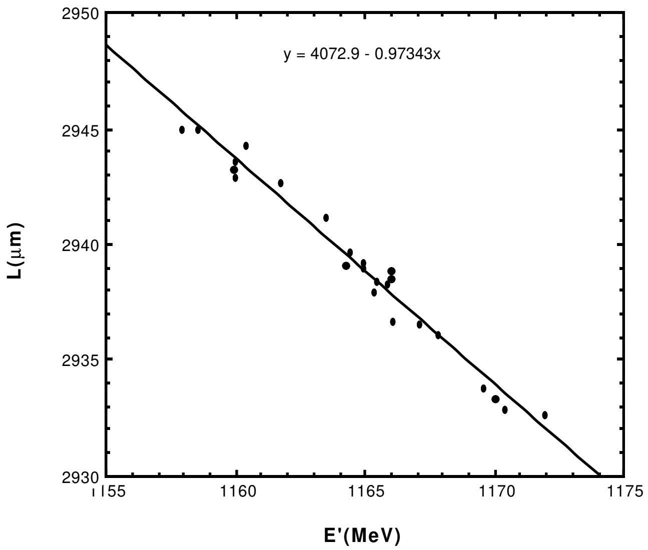

Figure 2. Relationship between absolute thickness (as measured at LBL) and residual energy of a penetrating argon beam for CRIS detector #8128.

As one check of consistency between the parameters, we note that the slope m = dL/dE' is fitted for energies around E'. Since k' and a' are also tuned for those energies, m*secθ should equal dR'/dE' = $a'k'E'^{a'-1}$. We find however that these two quantities differ by 1.4 %. Nevertheless, dead layer calculations seem to be robust; if we use ($a'k'E'^{a'-1}$*cosθ) instead of m to multiply $E_{missing}$ in the leading equation above, then we get $\delta L \approx 41.8$ μm for detector #8128.

There are around a dozen separate inputs that go into these calculations. The sensitivity of δL varies greatly with errors in the different parameters and measured values: see Table 1. We may ascribe this dilema to the method, which essentially consists of comparing two large numbers to measure a small residual.

input	$\Delta(\delta L)/\delta L$
θ	+ 0.03 %
L_o	+ 4.6
m	− 1.2
k	− 4.1
k'	+ 0.8
a	− 57.1
a'	+ 9.1
L_{air}	− 0.006
E'	− 2.7
ΔE	− 4.3
gain	− 5.9

Table 1. Sensitivity of δL to uncertainties in inputs. Column 1 lists which inputs were varied (separately) upward by 0.1 %. Column 2 lists the relative effect on the computed dead layer thickness. By "gain" is meant a general increase in all recorded energies due to calibration errors, including those energies used to make the linear fits of L_o and m in (L,E') space. It is clear that the coefficient a must be known very accurately.

An alternative, and simpler method of measuring dead layers on detector #8128 was tried at MSU. In a series of three consecutive runs, two different thicknesses of aluminum foil were placed in front of the thin-window face of the detector, and then the detector was flipped so that the beam entered its junction side. A degrader was used to reduce the beam energy to ≈ 1270 MeV, insuring that no ^{36}Ar nuclei passed completely through the detector. The same orientations and locations were maintained throughout: see Figure 3.

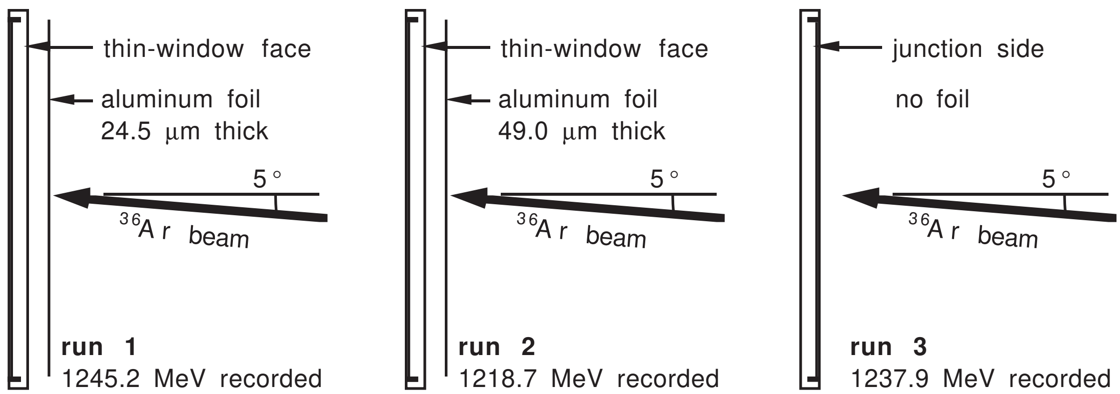

Figure 3. Setup for measuring dead layers on detector #8128 using foils.

The last run presents a dead layer (the detector junction) to the beam which we may consider to be like the foils in the earlier runs. The foil thicknesses of 1 mil (nominal) were corrected by weighing them (each with 180 cm^2 area) on a micro-gram balance. By linearly interpolating between the recorded energies, we find that the dead layer on the junction side of detector #8128 is thicker than that on the ohmic face by 31.3 µm of aluminum, which is equivalent to 35.0 µm of silicon.

This result should be quite believable. There is only one detector involved, and its thickness is irrelevant, so maps across its surface are unnecessary. Neither the beam energy nor the absolute gain needs to be known. (Our beam monitor recorded no significant shifts in energy between runs.) We do not even need to know the beam composition, so long as it did not vary. We can ignore all range-energy computations presented in the literature. (In fact, the predicted stopping power in aluminum is very close to that observed.) There are no airgaps to include. It is unlikely that charge-collection efficiency in the detector bulk depends on the side which particles enter. It is also unlikely that the foils were nonuniform.

The serious discrepancy between our two results is due to the complexity and sensitivity of the ΔE-E' method. Unfortunately, we could not map dead layers on all detectors by using some varient of the foil method. We might consider carefully re-tuning the ΔE-E' parameters.

ALPHA-PARTICLE MEASUREMENTS

The data which is most directly discrepant with the naive dead layer model is that taken with alpha particles. We radiated the junction side of CRIS detector #8092 with alphas from an encapsulated ^{228}Th source. These particles were collimated into an angle of less than 12° with respect to normal incidence. Measurements were made in a vacuum. Our results are listed here.

alpha I.D.	incident energy	range in silicon	ohmic-side peak position	junction-side peak position	junction:ohmic efficiency fraction
^{212}Po	8736 keV	56.7 μm	7721 ± 1 CH	3255 ± 20 CH	42 ± 0.3 %
^{216}Po	6723	36.9	5932 ± 1	1545 ± 20	26 ± 0.3
^{220}Rn	6231	32.7	5494 ± 1	1205 ± 30	22 ± 0.4
^{212}Bi	6004	30.9	5286 ± 1	1084 ± 45	21 ± 0.9
^{224}Ra	5636	28.0	4952 ± 1	845 ± 80	17 ± 1.6
^{228}Th	5323	25.7	4829 ± 2	705 ± 80	15 ± 1.7

Incident energies are known to within about 2 keV. Ranges are taken from J. F. Ziegler, Helium Stopping Powers and Ranges in All Elemental Matter (Pergamon, 1977). Pulser-determined offsets have been subtracted. The listed errors are conservative, and denote uncertainties on peak positions, not peak widths.

We assume that ohmic-side peaks correspond to complete collection of the incident energy. The naive dead layer model would then imply that since we recorded ≈ 3680 keV for ^{212}Po alphas entering the junction-side, dead layers must be around 42 μm thick. But this is contradicted by the collection of some ^{228}Th alpha energy. Suppose therefore that the charge collection efficiency is not zero, but constant through depth w, and unity beyond. The resulting partially-dead layer must be larger than 42 μm thick, else we would record more than 3680 keV for ^{212}Po alphas. We should then have collected the same fraction of deposited energy for all other alphas. Even allowing for significant errors in Ziegler's ranges we cannot obtain consistent results. Efficiency must vary within the junction.

Suppose the probability of collecting any charge depends only on its place of origin. To predict the average efficiency for free charges generated all along an alpha track (i.e. the fractions listed in the last column above), we must then convolute $\varepsilon(x)$ with the number of charges produced at each x; i.e. the known stopping power, dE/dx. As with the ranges, we take this latter function from Ziegler. For alpha energies above 1 MeV, the relative rate of energy loss is approximated quite well by $(dE(x)/dx)(R/E_o) \approx (1+a)(1 - x/R)^a$, where $a = -0.424$, R is the total range, and E_o is the incident energy: units are keV and μm. We then compute $\langle\varepsilon\rangle = \int_0^R \varepsilon(x)[dE(x)/dx]dx/E_o$.

Figure 4 shows a good fit between the alpha data and a linear model for $\varepsilon(x)$. This $\varepsilon(x)$ is not unique in its ability to match the data. Other functional forms were found to be equally good, but they implied rather different junction depths. We will present reasons below which argue for linearly varying charge collection efficiencies and junction depths in the range fitted here.

The average, effective dead layer thickness implied by the fit in Figure 4 is $\delta L \approx 41$ μm. This compares badly with $\delta L \approx 50$ μm implied by measurements made at MSU using foils. (Note, detector #8092 is one of only three detectors which were studied in this way with the ^{36}Ar beam: #8128 and #8138 were the others. We made auxiliary measurements with alphas for #8092 only.) This disagreement is not due to the functional form of $\varepsilon(x)$. Different relationships yielded very similar values for δL from the alpha data. We suspect that since 30 MeV/nucleon ^{36}Ar nuclei deposit energy in silicon at a rate that is 8 times higher than that for 1.5 MeV/nucleon alphas, then recombination is also higher and the average ε drops. We have not performed any other tests to confirm this.

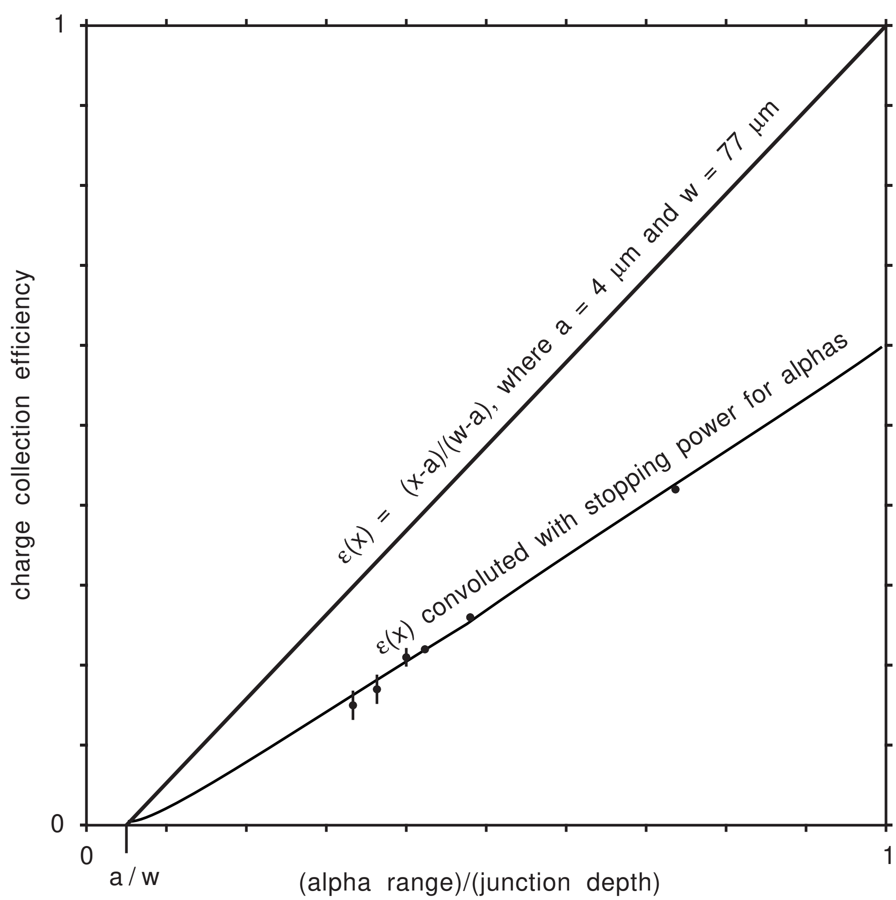

Figure 4. Fit to alpha data for detector #8092. The points indicate the fraction of alpha energy recorded versus range relative to a fitted junction depth of 77 μm.

THE SIMPLE DIFFUSION MODEL OF CHARGE COLLECTION

A uniquely specifiable model for $\varepsilon(x)$ can be intuited from a basic knowledge of free charge motion in silicon. At room temperature, electrons and holes move about at thermal velocities ($v \sim 20$ cm/μs), and mobility is limited by acoustic scattering off the crystal lattice, with mean free paths of order $\lambda \sim 0.1$ μm. The time it takes a charge to diffuse $\delta L \approx 100$ μm in projected distance is $\delta L^2/\lambda v \sim 0.5$ μs. Thus, holes generated inside the junction can diffuse out in time to be swept up by the electric field and contribute to our signal pulse. (We are concerned especially with holes, since electrons generated within the junction do not contribute to our signals.) Charges may diffuse toward the metallic contact, where they are absorbed, or to the high-field edge. At $x = 0$ the charge is lost, and does not add to signals. At $x = w$ the field takes over. Our problem then reduces to diffusion between two absorbing walls.

Charge carrier lifetimes in our CRIS silicon are measured in milliseconds, so trapping may be ignored in the crystal bulk. We assume for the moment that trapping and recombination is also negligible within the field-free junction.

If the diffusion length is the same throughout the junction, then $\varepsilon(x)$ is exactly linear, rising from 0 at $x = 0$ to unity at $x = w$. This linearity can be understood via the following argument. A hole walking randomly from its origin at $x = w/2$ has equal chances of being absorbed at $x = 0$ or else $x = w$, so $\varepsilon(w/2) = 1/2$. A hole generated at $x = w/4$ must first reach $x = w/2$ to get to $x = w$. But its chance of getting to $x = w/2$ before $x = 0$ is 1/2, so the probability of its reaching $x = w$ is $\varepsilon(w/4) = 1/2*\varepsilon(w/2) = 1/4$. By continuing such reasoning, we see that $\varepsilon(x) = x/w$ for all $0<x<w$. We refer to this as the "simple diffusion" model.

In fitting the alpha data for detector #8092, we found it necessary to introduce an offset; i.e. to assume $\varepsilon(x) = 0$ for the first 4 μm of silicon below the surface. We might speculate that this corresponds to a damaged region of the crystal, due to lapping, in which charge trapping is dominant. Alternatively, a force due to image charges in the metallic contact may attract such nearby holes to the surface. And yet another possibility exists: the diffusion time to reach $x = w$ may be just too long for holes generated this close to the surface to contribute to our signals. Whatever the dominant cause, we suspect that such offsets are a robust feature of any charge collection efficiency model. Indeed, other functional forms of $\varepsilon(x)$ seem to require similar offsets in order to acheive good fits.

We may quibble whether the simple diffusion model is correct. Maybe diffusion lengths are modified by the varying density of lithium in the junctions. Maybe recombination dominates for ionization produced by particles other than low-energy alphas. Maybe the cusp at $x = w$, where $\varepsilon(x)$ reaches unity, seems unphysical. However, the cogency of the model and the ease of making a good fit argue that it is worth keeping as a working hypothesis.

DETECTOR OPERATION AND JUNCTION FABRICATION

We will now spend a couple pages describing the workings of silicon detectors, and the fabrication of diffused junctions on lithiated crystals. The result will be a calculation of junction depths which closely match the fitted depth (w) suggested by our alpha data.

Easily ionized, or "shallow" impurities provide conductive charge within a semiconductor; with donors (acceptors) supplying electrons (holes) to n (p) "type" crystals. When an electric field E is introduced, each thermally activated free charge carrier drifts with average velocity $v_{drift} = \mu E$, where μ is its mobility. [The bulk resistivity is therefore $\rho = 1/q\mu\eta$, where η is the concentration of the dominant ("majority") impurity type. At room-temperature, and for $\eta < 10^{14}$ cc^{-1}, electron (hole) mobilities are ~ 1400 (400) cm^2/Vsec.] If a rectifying junction is present, then these carriers are driven out, not to be re-supplied (i.e. DC currents drop to miniscule levels), and a stable space-charge region of depth d develops, with charge density equal to the impurity concentration. By Gauss's law, the electric field falls linearly from $E_o = 2V/d$ to zero within such a "depleted" volume, where V is the applied voltage. Any other electron-hole pairs liberated in this high-field region (e.g. by a particle interaction) will be swept in opposite directions, and are detectable above the residual shot noise using suitable amplifying electronics. Thus, a planar ionization detector made using silicon has an active depth of $d = \varepsilon_{Si}E_o/q\eta = (2\varepsilon_{Si}V/q\eta)^{1/2}$, where ε_{Si} = 1.2 pF/cm is the dieletric constant. The device capacitance per unit area is $C/A = (q\eta\varepsilon_{Si}/2V)^{1/2}$.

The practical (manufacturing) limit of attainable silicon purity, in conjunction with good uniformity and carrier lifetime, is achieved for p-type crystals with dopant densities a bit less than 10^{12} acceptors/cc; which converts to room-temperature resistivities below about 20 kΩcm. The highest biases that can be applied are bounded by the dielectric breakdown characteristics of typical junctions to only a few hundreds of volts, which in turn are sensitively dependant upon fabrication techniques. Thus, silicon detectors of thicknesses beyond ~ 1 mm are not feasible; that is, without introducing further processing tricks.

Compared with other shallow donors, lithium has the best combination of solid solubility, diffusivity, ion mobility, and latttice stability. As an interstitial, it electrostatically binds with acceptors, forming electrically inactive dipoles. Carrier mobility and lifetime are not impaired by its presence. It is therefore used to "compensate" p-type silicon. Bulk crystals with effective resistivities of order 100 kΩcm can be created. Correspondingly thicker detectors are possible.

Jack Walton and others at LBL have developed successful methods to produce such devices. The essential steps used to make our CRIS detectors include ...

0) start with monocrystalline 1 - 3 kΩcm, p-type silicon (manufactured from Topsil)

1) deposit lithium by evaporation in a ≈ 375 °C vacuum for ≈ 1 minute

2) diffuse at ≈ 375 °C in an argon atmosphere for ≈ 15 minutes

3) drift at ≈ 110 °C for ~ 10^8 Vsec to fully compensate the 3 mm wafer

4) lap down the diffused junction until a four-point probe resistance of ≈ 20 Ω is reached

5) evaporate thin layers of Al and Au on the two detector faces to get good electrical contact

From these steps we can calculate the junction depth. We begin by noting that since the lithium is near its solubility limit in silicon throughout the diffusion process ($\eta_o \approx 6 \times 10^{17}$ cc^{-1}), then its initial density profile is a complementary error function: $\eta_{Li}(z) = \eta_o(1 - 2\int_0^z e^{-y^2} dy/\sqrt{\pi})$, where $z = x/2\sqrt{Dt}$, with t ≈ 15 min. This distribution is seen in Figure 5. The diffusion constant for lithium in silicon at ≈ 375 °C is $D \approx 1.65 \times 10^{-8}$ cm^2/sec. The lithium density equals the original acceptor concentration ($\eta_a \approx 4 - 13 \times 10^{12}$ cc^{-1}) at depth $w_o \approx 228 - 242$ µm.

When bias is applied in step 3) a subtle depletion region is formed. Beyond depth w_o the crystal is still p-type, whereas below w_o it is now dominated by lithium and so becomes n-type. The depletion region extends in both directions about this point a distance $d_\pm$ such that Gauss's law holds: $\varepsilon_{Si}E_o = q\left|\int_{w_o}^{d_\pm} \eta(x)dx\right|$, where $\eta(x) = \eta_{Li}(z) - \eta_a$.

The excess lithium in $x < w_o$ is free and mobile. Each such ion within the depletion region drifts under the influence of the electric field as an interstitial until it encounters an acceptor with which it binds. (We assume that our CRIS crystals are relatively free of any other kind of defect that inhibits transport.) A nearly perfect, one-to-one compensation is achieved thereby. Lithium is taken out of the region below w_o, and so the type-inversion point itself moves closer to the crystal surface, and the lithium profile becomes steeper there. Eventually, when $L\eta_a \approx \int_{d_\pm}^{w_o} \eta_{Li}(z)dx$ the whole wafer is compensated, where L = 3 mm. The type-inversion point has then moved back to a new position $w' \approx 154 - 172$ µm.

The average resistivity within the junction is $\rho_j^{-1} \approx q\int_0^w \mu\eta_{Li}(z)dx/w$. This is related to the measured four-point probe resistance R as $\rho_j = \pi Rw/\ln 2$. In step 4), the junction surface is lapped away until R ≈ 20 Ω. We calculate that about 100 µm of crystal is removed. The density of lithium at this surface is ≈ 3.7×10^{16} cc^{-1}, or a factor of almost 28 higher than that at the junction edge. The final junction depth is $w \approx 54 - 71$ µm.

The deposition of aluminum as a metallic contact adds negligibly to the physical junction.

The above calculation represents only an initial estimate of w. Due to thermal diffusion, junctions will continue to thicken, presumably in proportion to the square root of time. The room-temperature diffusion constant is $D \approx 10^{-14}$ cm^2/sec.

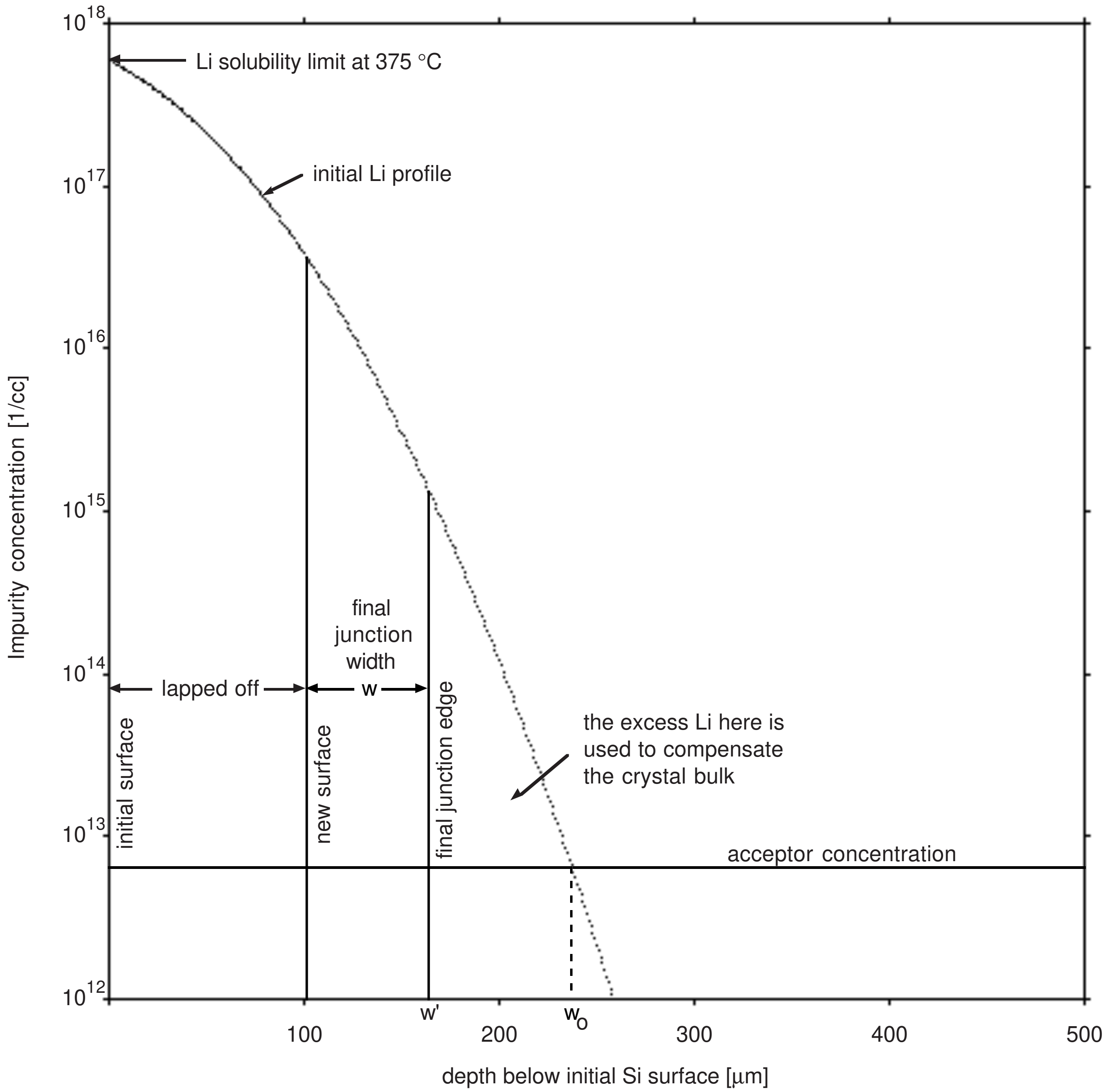

Figure 5. Calculated lithium profile during fabrication of the diffused junction.

CONCLUSIONS

We have uncovered a number of points that deserve further study. The "production" method used to calculate dead layer thicknesse maps is very sensitive to parameter errors, and should be carefully tuned. Charge collection efficiencies within the junctions are not zero, but vary with depth in an understandable (?) way. Effective dead layers may vary in thickness with the density of charge generated by an ionizing particle.